

Short communication

First-principles investigation of $\text{Mg}(\text{AlH}_4)_2$ complex hydride

Z.F. Hou

Department of Physics, Fudan University, Shanghai 200433, PR China

Available online 22 May 2006

Abstract

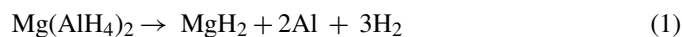
Within the framework of density functional theory, we investigate the structural properties, electronic structure, and the chemical stability of magnesium alanate ($\text{Mg}(\text{AlH}_4)_2$), a complex hydride for hydrogen storage, using the projector augmented plane wave method. The calculated structural properties of magnesium alanate compare well with the recent experiment. A detailed study of the electronic structure and charge density redistribution reveals the orbital hybridization and characteristics of bonding orbitals within the complex hydride. We found an ionic covalent bonding between Al and H in the $(\text{AlH}_4)^-$ anionic complexes embedded in the matrix of Mg^{2+} cations. The calculated reaction energy of $\text{Mg}(\text{AlH}_4)_2$ is in good agreement with the experimentally determined value.

© 2006 Elsevier B.V. All rights reserved.

Keywords: Hydrogen storage materials; Alanates; First-principles; Electronic structure

1. Introduction

The use of hydrogen-based energy in practical applications such as fuel cell vehicles requires the development of safe and efficient hydrogen storage technology. At present, there are three generic routes for the solid state storage of hydrogen [1,2]: (i) physisorption as in many porous carbon and zeolite materials with high specific surface area; (ii) hydrogen interaction in metal hydrides; (iii) chemical reaction such as in complex metal hydrides. Group 1, 2, and 3 light metals (e.g. Li, Mg, B, and Al) give rise to a large variety of metal–hydrogen complexes, which are especially interesting and have been attracted considerable attention because of their potential use as lightweight materials for reversible hydrogen storage [1]. Compared with LiAlH_4 and NaAlH_4 (with 10.6 and 7.5 wt.% theoretical hydrogen content, respectively), magnesium alanate ($\text{Mg}(\text{AlH}_4)_2$), is another potential hydrogen storage candidate with a hydrogen content of 9.3 wt.% [3]. This compound decomposes in a two-step reaction [3]:



where α and β in reaction (2) are Al–Mg solid solutions (such as Al_3Mg_2). Reaction (1) has been found to occur at temper-

atures of 135–163 °C [4–7] and reproduce 7.0 wt.% released hydrogen. The second reaction step has been reported that it completes with 2.3 wt.% released hydrogen and occurs at 270–310 °C [5,8]. However, the formation of stable MgH_2 as an intermediate or Al_3Mg_2 as an end product might negatively influence the reabsorption of hydrogen when starting from the respective dehydrogenated state of the material [7]. In order to improve the performance of $\text{Mg}(\text{AlH}_4)_2$ involved in reversible hydrogen absorption/desorption processes, understanding the fundamental physical properties of this complex hydride is of key importance and great interest.

Although theoretical investigations using the first-principles calculations are so common for alkali complex hydrides [2,9–11], only few studies on $\text{Mg}(\text{AlH}_4)_2$ has been reported, in which one [12] a variety of $\text{Mg}(\text{AlH}_4)_2$ clusters were served as models of the bulk structure and it is mainly concerned with the structural properties. The reaction enthalpy of hydrogen desorption for $\text{Mg}(\text{AlH}_4)_2$ is estimated as 41 kJ mol⁻¹ per H_2 molecule based on the cluster model [12] or as 46 kJ mol⁻¹ per H_2 molecule from ab initio vibration properties calculations based on density-functional perturbation theory [13], respectively, which are both much larger than the value of 0 kJ mol⁻¹ suggested in the review study [14] in light of the experimental measures [14,15].

Therefore, we employ first-principles approaches based on density functional theory and the projector augmented plane wave method to conduct a comprehensive study of the structural, electronic, and stability properties of $\text{Mg}(\text{AlH}_4)_2$. The system-

E-mail address: zfhoul@fudan.edu.cn.

atic analysis of the electronic properties of $\text{Mg}(\text{AlH}_4)_2$ suggests a covalent type of bonding between Al and H within the complex, but with a large ionicity. This is the generic bonding characteristics in alkali complex hydrides [9]. From the static total energy calculations, i.e. the zero-point energies are not included, we have obtained that a reasonable reaction enthalpy of hydrogen desorption for $\text{Mg}(\text{AlH}_4)_2$ is $-2.22 \text{ kJ mol}^{-1}$ which is in good agreement with the experimental value.

2. Computational methodology

First-principles calculations on $\text{Mg}(\text{AlH}_4)_2$ were performed using the Vienna ab initio simulation package (VASP) [16,17], which is based on the density functional theory (DFT) [18]. The generalized gradient approximation (GGA) of Perdew et al. [19] known as GGA-PW91 was used to treat the electronic exchange-correlation energy. Electron-ion interaction was represented by the projector augmented wave (PAW) method [20] with plane waves up to an energy of 550 eV. The reference configurations for valence electrons were $3s^23p^0$ for Mg, $3s^23p^1$ for Al, and $1s^1$ for H, respectively.

To examine the transferability of the pseudopotentials, the calculations have been performed on the related solid (Mg, Al, and MgH_2) and a H_2 molecule. We choose the rutile-type α - MgH_2 for simplicity. The same energy cutoff with GGA-PW91 is used. For solids, the k -point grids for Brillouin zone integration are generated according to the Monkhorst-Pack scheme [21] so as to make the edge lengths of the grid elements closer to the target value of 0.08 bohr^{-1} ($1 \text{ bohr} = 0.529 \text{ \AA}$) as possible. The same conditions are applied for the calculations on $\text{Mg}(\text{AlH}_4)_2$. The resulting k -point grid is $9 \times 9 \times 9$ (349 irreducible points) for hexagonal $\text{Mg}(\text{AlH}_4)_2$. We have carefully checked that these conditions give good convergence of the total energy within 1 meV atom^{-1} . The calculation for an isolated H_2 molecule is carried out using a cubic supercell with size of $15 \text{ \AA} \times 15 \text{ \AA} \times 15 \text{ \AA}$ and with the single Γ point for the k -point sampling. The results are given in Table 1. The lattice constants (interatomic distance), atomic positions and cohesive energies

Table 1
Results for hcp-Mg, fcc-Al, H_2 molecule and rutile-type α - MgH_2 , including the lattice constants a and c (in \AA), cohesive energy E_{coh} (in eV per formula unit), interatomic distance d (in \AA), and positions of H (u_{H}) atoms

Material	Property	This work	Experiment	Reference
hcp-Mg	a	3.18	3.21	[27]
	c	5.24	5.21	
	E_{coh}	1.48	1.51	
fcc-Al	a	4.04	4.05	[27]
	E_{coh}	3.49	3.39	
H_2	d	0.75	0.741	[28]
	E_{coh}	4.56	4.74	
α - MgH_2	a	4.495	4.501	[29]
	c	3.006	3.010	
	u_{H}	0.304	0.304	
	E_{coh}	6.70	–	

Note that the zero-point energies are not included in E_{coh} .

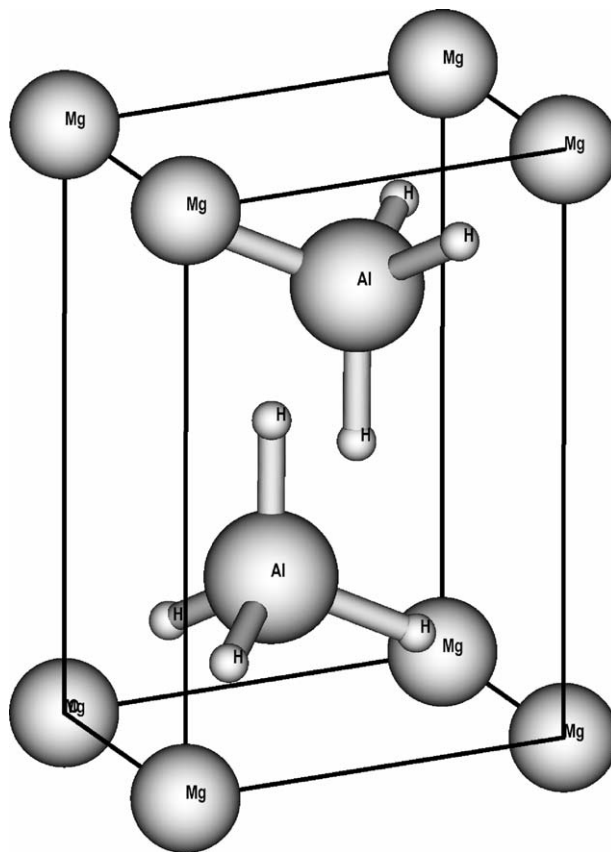


Fig. 1. Crystal structure of hexagonal $\text{Mg}(\text{AlH}_4)_2$.

of the related solid and molecule are in good agreement with the available experimental data.

3. Results and discussion

3.1. Crystal structure

$\text{Mg}(\text{AlH}_4)_2$ crystallizes in a hexagonal structure having the $P\bar{3}m1$ space group. The structure was confirmed by combined powder synchrotron X-ray and neutron diffraction [3,7]. The ball-and-stick model for crystal structure of $\text{Mg}(\text{AlH}_4)_2$ is illustrated in Fig. 1. The structure consists of isolated and slightly distorted AlH_4^- tetrahedra that are connected via six-coordinated Mg atoms in a distorted octahedral geometry, resulting in a sheet-like structure along the crystallographic c -axis [3]. Starting from experimentally available parameters, the lattice vectors of primitive cell and atomic coordinates were relaxed at a series of fixed volumes by optimizing both the forces and stresses. The residual force and stress in the equilibrium geometry are of the order of 1 meV \AA^{-1} and 10^{-3} GPa , respectively. The obtained energies were fitted with a Murnaghan equation of state [22] to give the equilibrium volume and the minimum energy. In order to further assess the effects of the exchange-correlation approximation on the structural properties the local density approximation (LDA) [23] and GGA of Perdew-Burke-Ernzerhof (PBE) parameterization [24] were also considered in addition to GGA-PW91. The final calculated cell parameters and

Table 2

Comparison between calculated and experimental lattice constants, internal parameters, and bond lengths for hexagonal $\text{Mg}(\text{AlH}_4)_2$ (space group $P\bar{3}m1$)

	This work			Experimental [3] (8 K)
	LDA	GGA-PW91	GGA-PBE	
Lattice constants (\AA)				
a	5.133	5.232	5.245	5.208
c	5.594	6.025	6.044	5.839
Volume (\AA^3)	127.64	142.86	144.01	137.16
Internal parameters				
Al_z	0.688	0.706	0.706	0.6991
H1_z	0.340	0.440	0.441	0.4242
H2_x	0.165	0.168	0.168	0.1671
H2_z	0.796	0.812	0.812	0.8105
Bond lengths (\AA)				
Mg–H2	1.86	1.90	1.91	1.870
Mg–Al	3.44	3.50	3.51	3.482
Al–H1	1.61	1.60	1.60	1.606
Al–H2	1.62	1.63	1.63	1.634

The Wyckoff positions of Mg, Al, H1, and H2 atoms are $1a$ (0, 0, 0), $2d$ ($1/3$, $2/3$, z), $2d$ ($1/3$, $2/3$, z), and $6i$ (x , $-x$, z), respectively. x and z are the fractional coordinates of the nonequivalent sites of Al and H atoms in $\text{Mg}(\text{AlH}_4)_2$.

bond lengths are given in Table 2, along with experimental values.

As seen in Table 2, GGA-PW91 and GGA-PBE consistently yields the larger volumes (4% and 5%, respectively) than experiment, which are typical for the GGA approximation to DFT. While LDA gives a smaller (7%) volume than that of experiment. We notice that GGA-PW91 also yields a better cell parameters of $\text{Mg}(\text{AlH}_4)_2$, including the lattice constants, positions of H atoms and the bond lengths. For example, the reported $\text{Mg}(\text{AlH}_4)_2$ lattice constants (at 8 K) [3] are 5.208 and 5.839 \AA , respectively, while we obtain 5.232 and 6.025 \AA . Our calculated Al position ($1/3$, $2/3$, 0.706) and H positions ($1/3$, $2/3$, 0.440) and (0.168, -0.168 , 0.812) are also in good agreement with the reported values [3].

3.2. Electronic structure

The energy band structure and electronic density of states (DOS) of $\text{Mg}(\text{AlH}_4)_2$ are calculated and shown in Figs. 2 and 3, respectively. Both of these figures exhibit a rather large energy gap of about 4.3 eV between valence and conduction bands, indicating that $\text{Mg}(\text{AlH}_4)_2$ is a wide-gap insulator. The eight valence bands in Fig. 2 have a width of about 6 eV and are split into two disjointed groups consisting of two and six bands, respectively. These two groups do not overlap in energy. From these figures it can be seen that the first two valence bands from -6 to -4 eV are derived from H s and Al s orbitals, while the next six bands in the higher-energy group between -3 and 0 eV are mainly from H s and Al p states. This suggests that there is a strong hybridization between H and Al orbitals. The conduction bands mainly by Mg (and to lesser extent Al) empty states. Mg has hardly any projection in the occupied states, while H has hardly any projection in the range of the empty states shown in Fig. 3. These features indicate that a highly ionic covalent bonding of hydrogen and

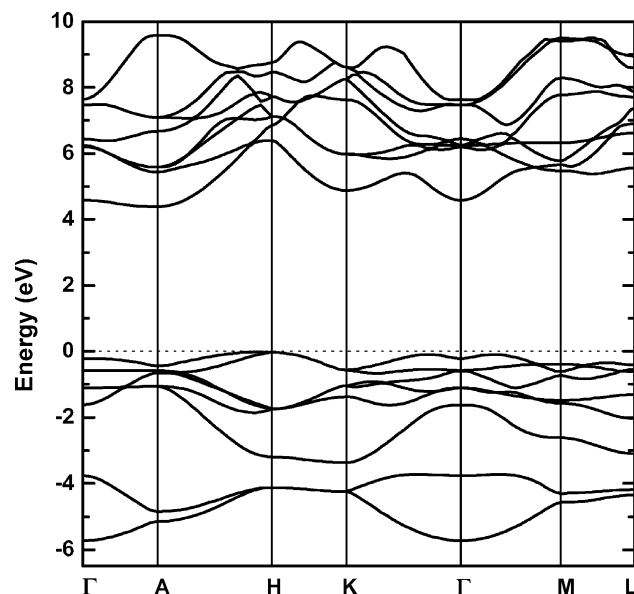


Fig. 2. Energy band structure of $\text{Mg}(\text{AlH}_4)_2$. The energy zero is set at the top of the valence band and shown as dotted line.

aluminum exists in the anion complex AlH_4^- . This characteristic bonding of complex AlH_4 has also been reported in NaAlH_4 compound [9].

In order to further analyze the bonding in $\text{Mg}(\text{AlH}_4)_2$, the charge distribution and charge transfer in the AlH_4 complexes are also examined. The total charge density $\rho(r)$ and the difference charge densities $\Delta\rho(r)$ in the plane containing Mg, Al, and H atoms, are shown in Fig. 4. The difference charge density $\Delta\rho(r)$ [9] is defined as the difference between the total charge density of the solid and a superposition of atomic charge densities with the same spatial coordinates as in the solid. In Fig. 4, the total charge density plot shows that the buildup of the electron density is mainly around the positions of H atoms and exhibits a slightly directional distribution toward Al atoms, while the difference density plot shows the charge transfer from Al to H

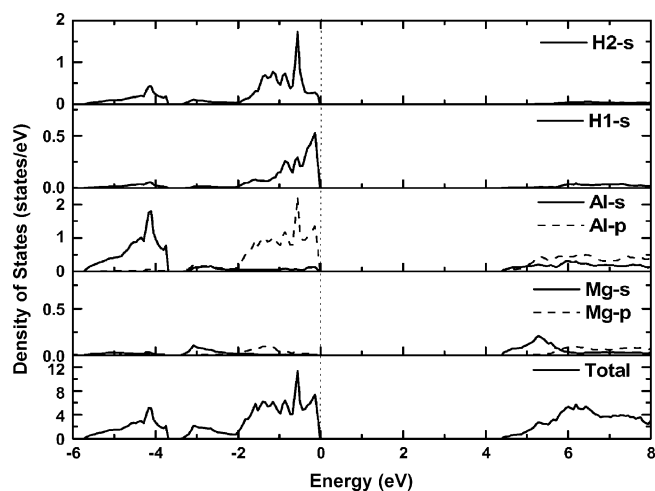


Fig. 3. Electronic density of states (DOS) of $\text{Mg}(\text{AlH}_4)_2$, including the total and projections DOS. The energy zero is set at the top of the valence band and shown as dotted line.

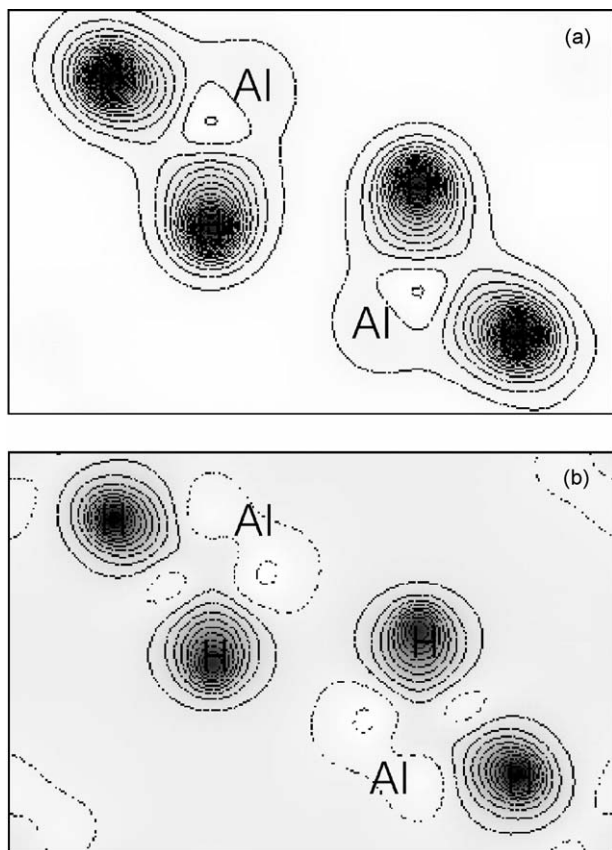


Fig. 4. Total and difference charge density plots of $\text{Mg}(\text{AlH}_4)_2$ in the (1 1 0) plane. (a) The total charge density represented by contours in an interval of 0.09 electrons \AA^{-3} from 0 to 1.87 electrons \AA^{-3} . (b) Charge deficiency in the difference plot is plotted in dashed lines, while the density increase near the hydrogen atoms is plotted in solid lines with an increment of 0.06 electrons \AA^{-3} from -0.108 to 0.63 electrons \AA^{-3} .

leaving aluminum positively and hydrogen negatively charged. These features support a covalent type of bonding but with a large ionicity in AlH_4 complexes.

3.3. Formation energy

The heat of formation is the most fundamental and important quantity for the hydrogen storage materials. For $\text{Mg}(\text{AlH}_4)_2$, the cohesive energy E_{coh} is calculated as 27.36 eV per formula unit. Using this value and the energies given in Table 1, the heat of formation for $\text{Mg}(\text{AlH}_4)_2$ is calculated according to the reaction as



If only the total energies are considered, the heat of formation for $\text{Mg}(\text{AlH}_4)_2$ is estimated as +0.63 eV per formula unit (i.e. -61.07 kJ mol^{-1}). In comparison, the heat of formation for $\alpha\text{-MgH}_2$ is obtained -63.36 kJ mol^{-1} , which is in excellent agreement with the previous theoretical study (-64 kJ mol^{-1} without zero-point energy contributions) [25] and in good agreement with the experiment value (-75.2 , -67.0 , -74.4 , and -65.8 kJ mol^{-1}) [26]. Following Eq. (1) which is more closely related to hydriding and dehydriding reactions, it is possible

to determine the reaction enthalpy of hydrogen desorption for $\text{Mg}(\text{AlH}_4)_2$. Therefore the reaction enthalpy of hydrogen desorption for $\text{Mg}(\text{AlH}_4)_2$ is predicted as -2.22 kJ mol^{-1} without the zero-point energies, which is also very close to the value of 0 kJ mol^{-1} H_2 reported in experiment [14,15]. It indicates that the thermodynamic properties of $\text{Mg}(\text{AlH}_4)_2$ appear to be unfavorable for reversible hydrogen storage under practical conditions [14] due to stable MgH_2 as an intermediate.

4. Conclusions

The structural, electronic and stability properties of $\text{Mg}(\text{AlH}_4)_2$ have been calculated and analyzed. Our calculated structural parameters including the lattice constants and internal parameters are in good agreement with the experiment results. Especially, the hydrogen positions in $\text{Mg}(\text{AlH}_4)_2$ are very close to the deuterium positions obtained in the neutron diffraction measurement at 8 K. The volume of the unit cell calculated with the LDA approximations is about 7% smaller than the experimental value. The best calculated volume for $\text{Mg}(\text{AlH}_4)_2$ is obtained with the GGA-PW91 approach. Detailed calculations of electronic structure suggest that the complex hydride $\text{Mg}(\text{AlH}_4)_2$ is an insulator with GGA energy band gap of 4.3 eV. The total and projected electronic DOS combined with the charge density plots indicate significant charge transfer leading to Mg^{2+} ions and negatively charged AlH_4 complex. The bonding within the AlH_4 complex involves the hybridization between Al and H orbitals, but shows a strong ionic character. Total energy calculations are used to estimate the enthalpy change in the chemical reactions associated with the hydration/dehydration processes. The calculated values are very close to the measured values in experiments.

Acknowledgments

The author acknowledges support from Shanghai Postdoctoral Science Foundation under Grant No. 05R214106. The work reported here was performed at High-end Computing Center of Fudan University.

References

- [1] A. Züttel, Mater. Today 6 (2003) 24.
- [2] J. Iñiguez, T. Yildirim, T.J. Udovic, M. Sulic, C.M. Jensen, Phys. Rev. B 70 (2004) 060101.
- [3] A. Fossdal, H.W. Brinks, M. Fichtner, B.C. Hauback, J. Alloys Compd. 387 (2005) 47.
- [4] E. Wiberg, R. Bauer, Z. Naturforsch. 7b (1952) 131.
- [5] T.N. Dymova, V.N. Konoplev, A.S. Sizareva, D.P. Aleksandrov, Russ. J. Coord. Chem. 25 (1999) 312.
- [6] E.C. Ashby, R.D. Schwartz, Inorg. Chem. 11 (1972) 925.
- [7] M. Fichtner, O. Fuhr, O. Kircher, J. Alloys Compd. 356–357 (2003) 418.
- [8] M. Fichtner, J. Engel, O. Kircher, O. Rubner, Mater. Sci. Eng. B 108 (2004) 42.
- [9] A. Peles, J.A. Alford, Z. Ma, L. Yang, M.Y. Chou, Phys. Rev. B 70 (2004) 165105.
- [10] A. Aguayo, D.J. Singh, Phys. Rev. B 69 (2004) 155103.
- [11] P. Vajeeston, P. Ravindran, A. Kjekshus, H. Fjellvåg, Phys. Rev. B 69 (2004) 020104.

- [12] M. Fichtner, J. Engel, O. Fuhr, A. Glöss, O. Rubner, R. Ahlrichs, *Inorg. Chem.* 42 (2003) 7060.
- [13] E. Spanó, M. Bernasconi, *Phys. Rev. B* 71 (2005) 174301.
- [14] F. Schüth, B. Bogdanović, M. Felderhoff, *Chem. Commun.* 20 (2004) 2249.
- [15] P. Clady, B. Bonnetot, J.M. Létoffé, *J. Therm. Anal.* 15 (1979) 119.
- [16] G. Kresse, J. Hafner, *Phys. Rev. B* 47 (1993) 558.
- [17] G. Kresse, J. Furthmüller, *Comput. Mater. Sci.* 6 (1996) 15.
- [18] W. Kohn, L.J. Sham, *Phys. Rev.* 140 (1965) A1133.
- [19] J.P. Perdew, J.A. Chevary, S.H. Vosko, K.A. Jackson, M.R. Pederson, D.J. Singh, C. Fiolhais, *Phys. Rev. B* 46 (1992) 6671.
- [20] P.E. Blöchl, *Phys. Rev. B* 50 (1994) 17953.
- [21] H.J. Monkhorst, J.D. Pack, *Phys. Rev. B* 13 (1976) 5188.
- [22] D. Murnaghan, *Proc. Natl. Acad. Sci. U.S.A.* 30 (1944) 244.
- [23] D.M. Ceperley, B.J. Alder, *Phys. Rev. Lett.* 45 (1980) 566.
- [24] J.P. Perdew, K. Burke, M. Ernzerhof, *Phys. Rev. Lett.* 77 (1996) 3865.
- [25] C. Wolverton, V. Ozolinš, M. Asta, *Phys. Rev. B* 69 (2004) 144109.
- [26] D.R. Lide, *CRC Handbook of Chemistry and Physics*, 83rd ed., CRC Press, New York, 2002.
- [27] C. Kittel, *Introduction to Solid State Physics*, sixth ed., Wiley, New York, 1986.
- [28] Y. Fukai, *The Metal-Hydrogen System*, vol. 21 of Springer Series in Material Science, Springer-Verlag, Berlin, 1993.
- [29] M. Bortz, B. Bertheville, G. Böttger, K. Yvon, *J. Alloys Compd.* 287 (1999) L4.